Supplementary information

Microfluidic fabrication of dual-functional hydrogel optical fibers with controlled swelling for simultaneous light transmission and ionic conductivity

Arti Singh[a,b] *and Jinhwan Yoon*[a]

[a]Department of Chemical Engineering, Center for Innovative Chemical Processes, Institute of Engineering, University of Seoul, 163 Seoulsiripdaero, Dongdaemun-gu, Seoul 02504, Republic of Korea

[b]Graduate Department of Chemical Materials, Institute for Plastic Information and Energy Materials, Sustainable Utilization of Photovoltaic Energy Research Center, Pusan National University, 2 Busandaehak-ro 63 Beon-gil, Geumjeong-gu, Busan 46241, Republic of Korea

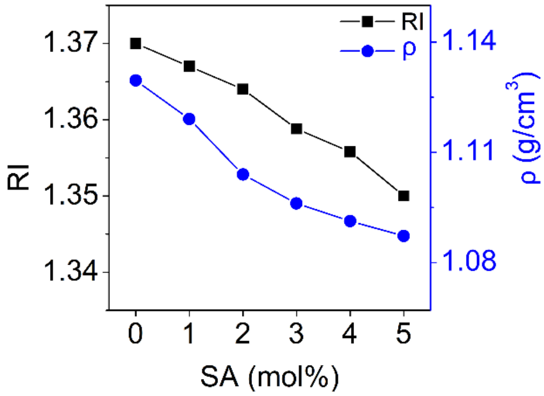

Fig. S1. Refractive index (black squares) and calculated density (blue circles) of swollen cladding as a function of sodium acrylate (SA) content (0–5 mol%).

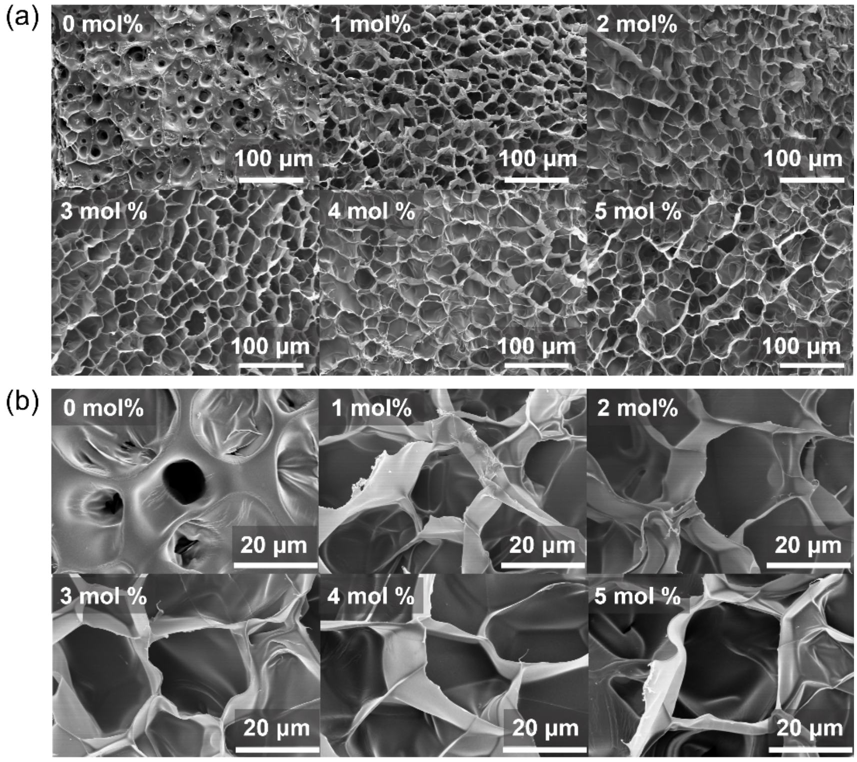

Fig. S2. Scanning electron microscopy images of freeze-dried cladding samples with 0-5 mol% SA content at (a) 100 µm and (b) 20 µm scale bars.

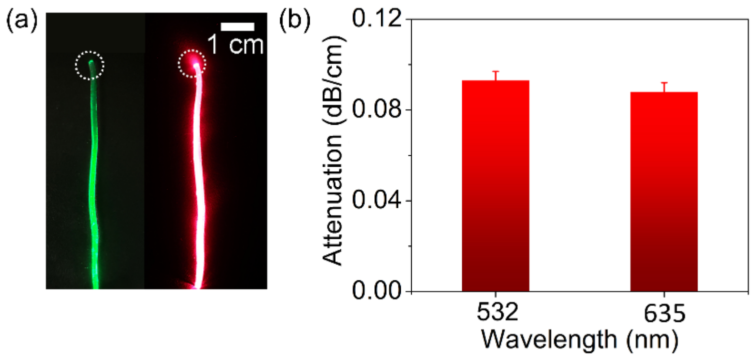

Fig. S3. (a) Light propagation photographs of CHOF (5 mol% SA) at 532 nm (green) and 635 nm (red). (b) Optical attenuation of CHOF (5 mol% SA) measured at 532 nm and 635 nm wavelengths.

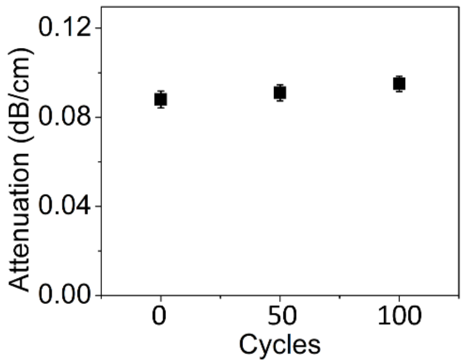

Fig. S4. Optical attenuation of CHOF (5 mol% SA) measured after repeated stretching cycles at 50% strain, showing stable performance over 100 cycles.

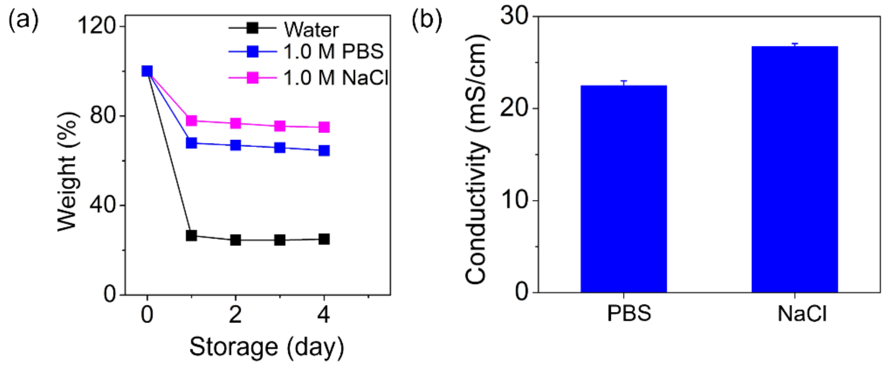

Fig. S5. Stability and conductivity in physiologically relevant solutions. (a) Weight stability of 5 mol% SA CHOFs over 4 days in water, 1.0 M PBS and 1.0 M NaCl. (b) Ionic conductivity in 1M PBS and NaCl solutions.

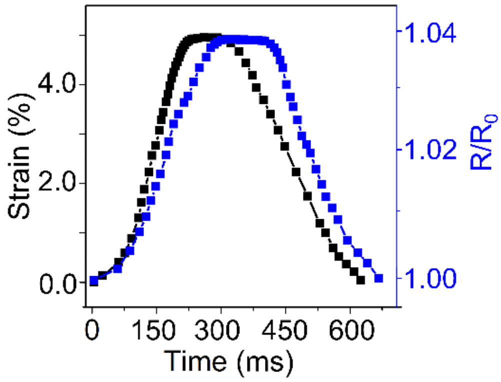

Fig. S6. Response time measurement during 5% strain application, showing applied strain (black, left y-axis) and normalized resistance change (blue, right y-axis).

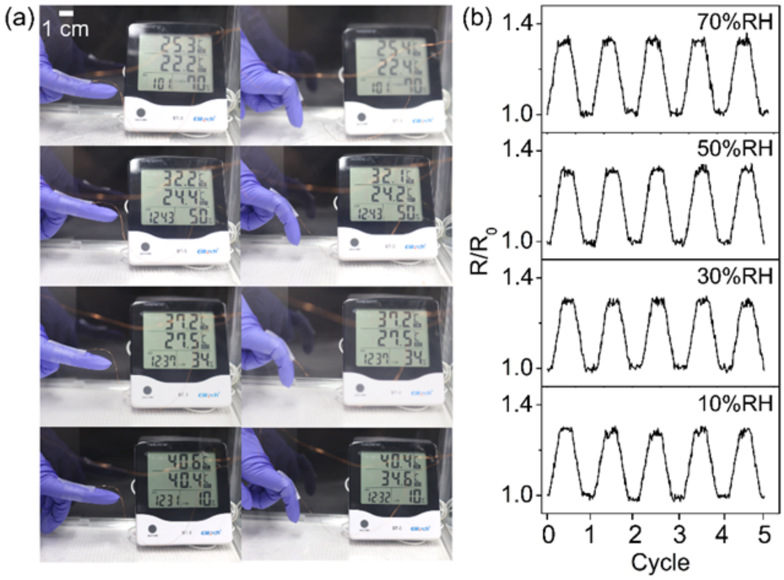

Fig. S7. Environmental stability under varying humidity conditions using 1.0 M NaCl. (a) Photographs showing finger motion detection at different RH levels (10%, 30%, 50%, 70%). (b) Resistance variation during finger motion at different RH conditions.

Table S1. Comparison of ionic conductivity in hydrogel ionic conductors reported in literature and this work.

Material system	Electrolyte (concentration)	Conductivity (mS/cm)	Reference
Gelatin/ Poly(ethylene glycol) diglycidyl ether	Potassium hydroxide (3.3M)	60	1
Hydroxyethylacrylamide /Chitosan	Lithium bis(trifluoromethanesulfonyl) imide (1 M)	39.4	2
Agar/ Polyacrylamide	Sodium chloride (1 M)	40	3
Poly(1-vinyl-3-butyl imidazolium bromide / Poly(vinyl pyrrolidone)	Lithium bromide (1 M)	26	4
Hydroxyethylacrylamide / Polydimethylsiloxane	Lithium chloride (1 M)	25.0	5
Carboxymethyl chitosan / Epichlorohydrin	Calcium chloride (4 M)	82	6
Poly(N-isopropylacrylamide)/Chitosan	Lithium bis(trifluoromethanesulfonyl) imide (1 M)	25.0	7
Polyacrylamide / Hydroxyethylacrylamide	Lithium bis(trifluoromethanesulfonyl) imide (1 M)	19.5	8
Polyacrylamide / Sodium acrylate	Sodium chloride (1 M)	26.6	*This work*

References

1. J. Wang, C. Gao, P. Hou, Y. Liu, J. Zhao and P. Huo, *Chem. Eng. J.*, 2023, **455**, 140952.
2. Y. Zhu, A. Hong, S. Y. Yoon, J. Park, H. Yang, J. Kwak and J. Yoon, *Small*, 2024, **20**, 2400704.
3. W. Hou, N. Sheng, X. Zhang, Z. Luan, P. Qi, M. Lin, Y. Tan, Y. Xia, Y. Li and K. Sui, *Carbohydr. Polym.*, 2019, **211**, 322–328.
4. X. He, T. Zhuang, S. Ruan, X. Xia, Y. Xia, J. Zhang, H. Huang, Y. Gan and W. Zhang, *Chem. Eng. J.*, 2023, **466**, 143209.
5. J. Park, S. Singh and J. Yoon, *Small*, 2025, **21**, 2502435.
6. C. Zhao, X. Gong, L. Shen, Y. Wang and C. Zhang, *ACS Appl. Polym. Mater.*, 2022, **4**, 4025–4034.

7. G. Fitria and J. Yoon, *J. Polym. Sci.*, 2022, **60**, 1758–1766.
8. Y. Go, H. Y. Park, Y. Zhu, K. Yoo, J. Kwak, S. H. Jin and J. Yoon, *Adv. Funct. Mater.*, 2023, **33**, 2215193.